A constitutive law for the viscous and tertiary creep responses of ice to applied stress

L.W. Morland[a], R. Staroszczyk[b],[*]

[a] School of Mathematics, University of East Anglia, Norwich NR4 7TJ, United Kingdom
[b] Institute of Hydro-Engineering, Polish Academy of Sciences, ul. Kościerska 7, 80-328 Gdańsk, Poland

A B S T R A C T

Given the initial (secondary creep) viscous response of ice to applied stress, the subsequent tertiary creep is described by an orthotropic fabric evolution relation motivated by crystal rotation arguments. That is, the ice is described as a non-simple anisotropic fluid with dependence on the evolving deformation. Extension and modification of previous formulations are proposed, in which a general orthotropic flow law for stress includes terms which are quadratic functions of the strain-rate tensor, compared to previously analysed relations in which only linear in the strain-rate tensor terms were considered. Ice response functions in the extended law are constructed in such a way that the validity equalities and inequalities between the instantaneous directional viscosities at each stage of the tertiary creep are satisfied, and correlations with families of idealised uni-axial and simple shear tertiary creep curves for different applied stresses are possible. It is shown for a range of free parameters in the proposed orthotropic model how accurately the assumed uni-axial and shear creep curves can be approximated by the constructed response functions.

1. Introduction

The flow of ice sheets plays an important part in climate change modelling, and a key element is the constitutive relation for a large ice polycrystal (the continuum element) formed at the surface as it moves through the sheet. The response to applied uni-axial stress exhibits a small primary deformation with rapidly decreasing strain-rate to a minimum strain-rate, referred to as secondary creep, followed by a tertiary creep with significantly increasing strain-rate to an asymptotic limit. The tertiary creep for applied shear stress shows a significantly decreasing strain-rate to a different asymptotic limit. This pattern of response has been modelled empirically as viscoelastic solids of differential type and of integral type and, ignoring the very small primary deformation, as viscoelastic fluids of differential type (Spring and Morland, 1982, 1983; Morland and Spring, 1981), but with no correlation with families of responses to different stresses, and no reference to any underlying crystal behaviour and the resulting fabric evolution with induced anisotropy. The ratios of the asymptotic limits to the initial strain-rates for uni-axial and shear responses are described as enhancement factors.

At the surface of an ice-sheet it is supposed that the basal glide planes of the many individual crystals within the polycrystal are randomly distributed, so that the initial viscous response, ignoring the

small primary deformation, is isotropic; that is, the ice behaves like a simple viscous fluid. During the subsequent deformation as the ice descends through the sheet, the crystals rotate differentially and so respond differently to an applied stress. Ice core samples taken from depth in an ice-sheet reveal strong fabrics, shown by significant alignment of initially randomly distributed c-axes of individual crystals, and consequent substantial differences in shear viscosities in different planes. Assuming that the glide resistance, viscosity, increases as the glide plane rotates away from the maximum shear traction direction, Morland and Staroszczyk (2009) integrated the resistance over all basal plane orientations during uni-axial and simple shear deformations to deduce the shapes, not magnitude, of the consequent tertiary creep curves, which are consistent with the accepted forms. This supports the previous rotation arguments used to formulate a general orthotropic constitutive relation describing the tertiary creep (Morland and Staroszczyk, 1998; Staroszczyk and Morland, 2000). Ice is very closely incompressible even at the very high pressures at the base of a large ice-sheet, so the pressure is a workless constraint determined by the momentum balance and boundary conditions, and the deformation is governed by a constitutive law for the deviatoric stress. Here we are focussing on a continuum description which ignores fracture and calving, and possible re-crystallisation at the bed, with the view that nearly all of a large cold ice-sheet will be governed by the continuum

* Corresponding author.
E-mail address: rstar@ibwpan.gda.pl (R. Staroszczyk).

law. In any case, the latter is required as a basis for fracture and re-crystallisation criteria.

Alternative methods to the phenomenological approach followed in this paper, in which the macroscopic stress in polycrystalline ice is described in terms of the macroscopic strain and strain-rate, are the theories in which the macroscopic behaviour of ice is derived from the properties and behaviour of individual ice crystals. Examples of such macro-macroscopic approaches, based on the concept of a so-called orientation distribution function (*ODF*) that defines continuous weightings to the ice crystal orientations in space at a given material point, are the models formulated by Svendsen and Hutter (1996), Meyssonnier and Philip (1996), Gödert and Hutter (1998) and Gagliardini and Meyssonnier (1999). Comparisons of the continuum and *ODF*-based macro-macroscopic model predictions were presented by Staroszczyk and Gagliardini (1999). Later, more complex theories, developed by employing the general principles of thermodynamics, were due to Faria et al. (2003) and Faria (2006). Various aspects of the modelling of evolving anisotropy of polycrystalline ice were reviewed by Placidi et al. (2006).

The initial incompressible isotropic viscous fluid response is described here by a general frame indifferent quadratic relation, with response coefficients depending on two strain-rate invariants, but here we suppose dependence on a single invariant, the second principal invariant. For illustration we adopt the customary co-axial relation between deviatoric stress and strain-rate, using the data correlation by Smith and Morland (1981) of Glen's (1955) uni-axial stress data for the strain-rate formulation, but here accurately inverted for a stress formulation. Additionally, we suppose the ice is thermorheologically simple, with all rates scaled by a temperature dependent factor.

Supposing that the response during the subsequent deformation phase is primarily a consequence of crystal rotation, ignoring any re-crystallisation, Morland and Staroszczyk (1998) used rotation arguments to deduce that the response is symmetric with respect to the current principal stretch planes. That is, the material has orthotropic symmetry with respect to the principal stretch planes which change continuously with the deformation, with consequent changing induced anisotropy described as fabric evolution. The stress then depends on orthotropic structure tensors and at least on the strain-rate and the deformation. There is a general algebraic relation for such orthotropic response, and a minimal form was adopted to explore the evolution of anisotropy, which was described by defining instantaneous directional viscosities which evolve with the fabric evolution. Subsequently Staroszczyk and Morland (2000) determined a set of equalities and inequalities (described by Morland as the *Staroszczyk Equalities and Inequalities*, now abbreviated to *SEI*), which must be satisfied by the directional viscosities at each stage of the fabric evolution, and proposed a new law involving two response functions depending on a shear deformation magnitude invariant and on the three principal stretches. It was found that one of the *SEI* equalities related the two response functions, leaving only one independent response function to correlate with data. A modified formulation involving two response function coefficients, in both stress and strain-rate formulations, was proposed by Morland and Staroszczyk (2003), with dependence on more convenient forms of invariants, but again the same *SEI* equality related the two response functions.

Here we now include all the terms of the general orthotropic law which define a non-simple fluid, depending on the evolving deformation, and which influence the shear response. To allow useful correlations with the tertiary uni-axial and shear responses, we adopt a simplified dependence on only one isotropic strain-rate invariant and one isotropic deformation invariant, and on three orthotropic deformation invariants. Different to previously analysed relations, we now include the initial viscous relation with an isotropic deformation-dependent weighting factor, and include an isotropic deformation-dependent weighting factor for the orthotropic terms. It will be seen that these weighting factors are necessary for approximate correlations with

tertiary uni-axial and shear responses.

With this form, we examine all the *SEI* to show that their validity can only be confirmed analytically if the isotropic deformation term is excluded, and the orthotropic response function has a particular shape. With these restrictions, we examine laterally confined simple shear response to constant shear stresses and investigate how it can be correlated approximately with an idealised family of monotonic tertiary creep curves at different constant shear stresses. We then analyse the uni-axial compression response to constant applied uni-axial stress and show that correlation with an idealised family of monotonic tertiary creep curves at different constant uni-axial stresses leads to a difference equation, not algebraic, for the orthotropic response coefficients, with no analytic solution.

We therefore assume a family of orthotropic response functions which satisfy all the *SEI* validity conditions, and determine the relations for the response coefficients and weighting factors given by shear correlations at the minimum and maximum initial strain-rates, and by the uni-axial correlations at the minimum and maximum initial strain-rates, anticipating that the tertiary responses at the interim initial strain-rates will be of similar shape and lie between the limit curves.

2. Temperature dependence

Ice response is strongly temperature T dependent and is assumed to be thermorheologically simple (Schwarzl and Staverman, 1952; Morland and Lee, 1960), in which the same processes occur, but on a time-scale factored by $a(T)$. Smith and Morland (1981) constructed exponential representations for the rate factor $a(T)$ over different temperature ranges from the constant uni-axial stress data (Mellor and Testa, 1969), and that with the widest validity is

$$a(T) = 0.7242 \exp(11.9567\overline{T}) + 0.3438 \exp(2.9494\overline{T}), \tag{2.1}$$

$$T = T_0 + 20^o \text{ K } \overline{T}, \quad T_0 = 273.15^o \text{ K}, \tag{2.2}$$

where T_0 is the melting point and $a(T_0) = 1.068$ is approximately unity, normalising the factor at the melt point. At 2° K below melting a $(271.15) = 0.4751$, less than half that at the melt point, and at 30° K below the melt point, a temperature magnitude found in cold ice-sheets, $a(243.15) = 0.0041$, implying much smaller strain-rates than those near melting.[1]

This temperature dependence is incorporated by relating the strain-rate $\mathbf{D}$ to a "temperature independent" strain-rate $\overline{\mathbf{D}}$ through the scaling

$$\mathbf{D} = a(T)\overline{\mathbf{D}}, \quad \text{trace}(\mathbf{D}) = 0, \quad I = \frac{1}{2}\text{trace}(\mathbf{D}^2) = \frac{1}{2}[a(T)]^2 \text{trace}(\overline{\mathbf{D}}^2)$$

$$= [a(T)]^2 \overline{I}, \tag{2.3}$$

where the second relation is the incompressibility condition, and the third relation defines the negative of the second principal invariant I of the strain-rate tensor, which is a measure of the shear strain-rate magnitude squared. Since the third invariant of the strain-rate tensor, $I_3 = \det(\mathbf{D})$, is not used, the usual subscript $_2$ is omitted. The strain-rate dependence in the constitutive relations is now expressed in terms of $\overline{\mathbf{D}}$ with the actual strain-rate at a non-melt temperature given by $(2.3)_1$.

3. Initial viscous response

When stress is applied to a large ice polycrystal, there is a small elastic or viscoelastic deformation which is considered unimportant over the long time-scales of ice-sheet flow, so the instantaneous

---

[1] We appreciate the advice given to us by Dr. David Cole who has examined many data sets for temperature variation and judges the Mellor and Testa (1969) data to show a consistent variation with temperature, though with higher strain-rates. The above $a(T)$ variation is therefore consistent, here normalised at the melt temperature T_0.

response is assumed to be that of a viscous fluid, necessarily isotropic by frame indifference, followed by a tertiary creep involving crystal rotation which induces anisotropy. Ice is incompressible, so the mean pressure p is a constraint determined by momentum balance and boundary conditions. The required viscous fluid relation for the deviatoric stress $\hat{\sigma}$ is defined by

$$\hat{\sigma} = \sigma + p\mathbf{I}, \quad p = -\frac{1}{3}\text{trace}(\sigma), \quad \text{trace}(\hat{\sigma}) = 0, \tag{3.1}$$

where $\hat{\sigma}$ is the Cauchy stress, in terms of the strain-rate $\overline{\mathbf{D}}$. Here the stress and strain-rate are dimensionless variables with respective units $\sigma_0 = 10^5$ Pa and strain-rate unit $D_0 = \text{a}^{-1}$, where 'a' denotes year, which are the deviatoric stress and strain-rate magnitudes expected, at melt point, in ice-sheet flow.

With the simplification that the response functions depend on only one-strain-rate invariant $\overline{I}$, the general frame indifferent viscous fluid expansion becomes

$$\hat{\sigma} = \phi_1(\overline{I})\overline{\mathbf{D}} + \phi_2(\overline{I})\left[\overline{\mathbf{D}}^2 - \frac{2}{3}\overline{I}\mathbf{I}\right], \quad \overline{I} = \frac{1}{2}\text{trace}(\overline{\mathbf{D}}^2), \tag{3.2}$$

where $\mathbf{I}$ is the unit tensor. Materials obeying the constitutive law (3.2) are usually referred to as Reiner-Rivlin fluids (Reiner, 1945; Rivlin, 1947). Morland and Staroszczyk (2019) examined in detail the instantaneous[2] viscous response data from combined stress experiments reported in Budd et al. (2013), which showed that the quadratic term is not zero. While incomplete measurements were replaced by an approximation, the data does suggest that the quadratic term is significant; that is, the response coefficient $\phi_2(\overline{I})$ is not zero, and the viscous relation (3.2) is not co-axial as commonly assumed. Note that the rate factor $a(T)$ does not then appear simply as a factor on $\hat{\sigma}$ as it does for the linear co-axial law. However, the Budd et al. (2013) data was inconsistent, and different sets of data points determined very different response functions, so no convincing relation was determined.

For our present analysis of fabric evolution laws which satisfy the *SEI* and can be correlated with uni-axial and shear tertiary response, and which depend on the initial viscous response, we will adopt an initial viscous co-axial relation determined by Smith and Morland (1981) from a close correlation with Glen's (1955) uni-axial compression data. This was determined for the inverse form

$$\overline{\mathbf{D}} = \psi(J)\hat{\sigma}, \quad J = \frac{1}{2}\text{trace}(\hat{\sigma}^2), \tag{3.3}$$

with

$$\psi(J) = c_0 + c_1 J + c_2 J^2, \quad c_0 = 0.3336, \quad c_1 = 0.32, \quad c_2 = 0.02963. \tag{3.4}$$

Since $\phi_2 = 0$ we set $\phi_1 = \phi$, then (3.3) and (3.4) imply

$$\phi(\overline{I})\psi(J) = 1, \quad \phi(0) = c_0^{-1} = 2.9976, \quad \mu_0 = c_0^{-1}/2 = 1.4988, \tag{3.5}$$

$$\overline{I} = \psi^2(J)J \sim c_2^2 J^5 \quad \text{for large } J \to J \sim c_2^{-2/5}\overline{I}^{1/5} \quad \text{for large } \overline{I}. \tag{3.6}$$

The Smith and Morland (1981) expansion choices for the correlations of ϕ took no account of the zero and large $\overline{I}$ conditions, and so were not good. Incorporating these conditions, we consider an n-term expansion with coefficients d_k ($k = 1, ..., n$) to be determined by a least squares correlation with $\psi^{-1}(J)$ using relations (3.5) and (3.6), namely

$$\phi(\overline{I}) = c_2^{-1/5}(d_1^2 + \overline{I})^{-2/5} + \sum_{m=2}^{n} d_m(d_1^2 + \overline{I})^{-(m+1)/5} + Z(d_1^2 + \overline{I})^{-(n+2)/5}, \tag{3.7}$$

$$Z = (d_1^{2(n+2)/5})/c_0 - c_2^{-1/5}d_1^{2n/5} - \sum_{m=2}^{n} d_m d_1^{2(1+n-m)/5}. \tag{3.8}$$

---

[2] Commonly described as the minimum strain-rate before tertiary creep starts, as arises in uni-axial stress tests, but is the maximum strain-rate in shear stress response.

A close correlation was determined with $n = 3$, for which the coefficients are

$$d_1 = 0.3401, \quad d_2 = -0.6527, \quad d_3 = -0.5522, \tag{3.9}$$

and Fig. 1 shows the close comparison of the reciprocal of this correlated $\phi(\overline{I})$ with $\psi(J)$.

4. Fabric evolution

The tertiary creep following the instantaneous viscous response involves crystal rotation, described as fabric evolution. This is accompanied by induced anisotropy which can be measured by the instantaneous directional viscosities associated with each stage of the deformation. Let $\mathbf{B}$ denote the symmetric left Cauchy-Green tensor which measures the deformation, and let b_1, b_2, b_3 be the ordered principal stretches squared acting along the principal directions defined by the unit vectors $\mathbf{e}^{(1)}$, $\mathbf{e}^{(2)}$, $\mathbf{e}^{(3)}$; thus

$$\mathbf{Be}^{(r)} = b_r\mathbf{e}^{(r)}, \quad \det(\mathbf{B} - b_r\mathbf{I}) = 0, \quad (r = 1,2,3), \quad b_1 \geq b_2 \geq b_3 > 0, \tag{4.1}$$

with strict inequalities except when the ice is in an undeformed isotropic state $\mathbf{B} = \mathbf{I}$, $b_1 = b_2 = b_3 = 1$. By ice incompressibility,

$$\det \mathbf{B} = b_1 b_2 b_3 = 1, \quad b_1 \geq 1, \quad b_3 \leq 1, \tag{4.2}$$

but the sign of $(b_2 - 1)$ is not fixed. That is, we assume that the maximum compression is in the $\mathbf{e}^{(3)}$ direction, and the maximum extension is in the $\mathbf{e}^{(1)}$ direction.

At a given deformation $\mathbf{B}$, a given fabric state, consider a simple shearing in the $\mathbf{e}^{(r)}$ direction on a plane normal to a distinct $\mathbf{e}^{(s)}$ direction. The instantaneous viscous response is defined by a directional viscosity μ_{rs} introduced by Morland and Staroszczyk (1998) which measures half the ratio of the corresponding components of the applied shear stress $\hat{\sigma}$ and strain-rate $\overline{\mathbf{D}}$, namely

$$\mu_{rs} = \frac{1}{2}\hat{\sigma}_{rs}/\overline{D}_{rs}, \quad \mu_0 = \frac{1}{2}\phi_1(0), \tag{4.3}$$

where μ_0 is the isotropic ice viscosity when $\mathbf{B} = \mathbf{I}$. From the underlying rotation concepts a set of equalities and inequalities between the directional viscosities μ_{rs} for the six possible ranges of ordered b_1, b_2, b_3 was subsequently derived in Staroszczyk and Morland (2000), named by Morland as the *Staroszczyk Equalities and Inequalities, SEI*. These are

$$b_1 = b_2 = b_3 = 1: \quad \mu_{ij} = \mu_0 \quad (i,j = 1,2,3), \tag{4.4}$$

$$b_1 = b_2 > 1 > b_3: \quad 0 < \mu_{13} = \mu_{23} < \mu_{12}, \tag{4.5}$$

$$b_1 > b_2 > 1 > b_3: \quad 0 < \mu_{13} < \mu_{23} < \mu_{12}, \tag{4.6}$$

$$b_1 > b_2 = 1 > b_3: \quad 0 < \mu_{13} < \mu_{23} = \mu_{12}, \tag{4.7}$$

$$b_1 > 1 > b_2 > b_3: \quad 0 < \mu_{13} < \mu_{12} < \mu_{23}, \tag{4.8}$$

$$b_1 > 1 > b_2 = b_3: \quad 0 < \mu_{13} = \mu_{12} < \mu_{23}. \tag{4.9}$$

The six relations (4.4)–(4.9) are based on the following assumption: the smaller a given principal stretch is compared to the other two stretches, the stronger is the alignment of crystal c-axes (the axes of crystal rotational symmetry) towards the direction of this stretch and, therefore, the easier is the crystal basal shearing on the principal plane normal to this principal stretch axis (that is, the smaller is the corresponding instantaneous shear viscosity). Although the six equalities and inequalities have been deduced by ignoring the local behaviour (interactions) of individual crystals and have not been confirmed experimentally, it is supposed here that a valid constitutive law for the macroscopic behaviour of polycrystalline ice must satisfy the set of relations (4.4)–(4.9).

We now modify and extend the orthotropic relations proposed by Morland and Staroszczyk (1998), Staroszczyk and Morland (1999, 2000) and Morland and Staroszczyk (2003), see also Staroszczyk
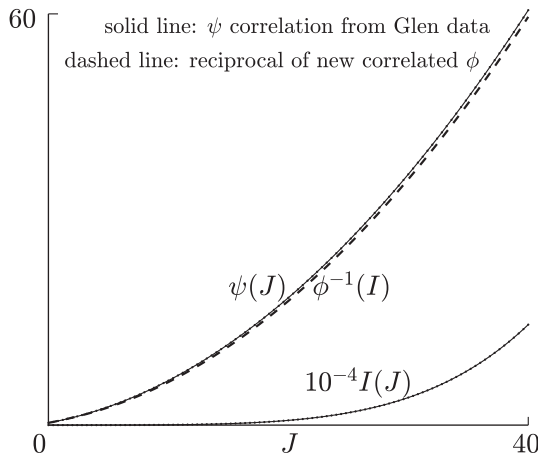
Fig. 1. The viscous response coefficients $\psi(J)$ and $\phi(\bar{I})$.

(2019), based on the general relations derived by Boehler (1987). These introduce weighting factors which depend on an isotropic deformation invariant η in order to allow correlation with tertiary uni-axial and shear responses at minimum and maximum initial strain-rates. The orthotropic symmetry is governed by orthotropic structure tensors $\mathbf{M}^{(r)}$, $(r = 1,2,3)$ with orthotropic invariants ξ_r. Thus,

$$\hat{\sigma} = \alpha(\eta)\left\{\phi_1(\bar{I})\overline{\mathbf{D}} + \phi_2(\bar{I})\left[\overline{\mathbf{D}}^2 - \frac{2}{3}\bar{I}\,\mathbf{I}\right]\right\}$$
$$+ c(\eta)\overline{\mathbf{D}} + h(\eta)\left[\overline{\mathbf{D}}^2 - \frac{2}{3}\bar{I}\,\mathbf{I}\right]$$
$$+ g(\eta)\left[\overline{\mathbf{D}}\mathbf{B} + \mathbf{B}\overline{\mathbf{D}} - \frac{2}{3}\text{tr}\,(\overline{\mathbf{D}}\mathbf{B})\mathbf{I}\right]$$
$$+ \delta(\eta)\sum_{r=1}^{3}f(\xi_r)\left[\mathbf{M}^{(r)}\overline{\mathbf{D}} + \overline{\mathbf{D}}\mathbf{M}^{(r)} - \frac{2}{3}\text{tr}\,(\mathbf{M}^{(r)}\overline{\mathbf{D}})\mathbf{I}\right],$$
$$(4.10)$$

where $\mathbf{M}^{(r)}$ $(r = 1,2,3)$ are orthotropic structure tensors, and ξ_r and η are orthotropic and isotropic invariants, respectively, defined by

$$\mathbf{M}^{(r)} = \mathbf{e}^{(r)} \otimes \mathbf{e}^{(r)}, \quad \xi_r = b_r - 1/b_r, \quad (r = 1,2,3),$$
$$\eta = \sqrt{(K-1)^2 - 4}, \quad K = \text{tr}\,\mathbf{B}. \quad (4.11)$$

The quadratic term in $\overline{\mathbf{D}}$ with weighting $h(\eta)$ in (4.10) is the extra term compared to the previous formulation (Staroszczyk and Morland, 2000), and is introduced to allow better correlation with uni-axial response. This choice of deformation invariant η implies

$$\eta \geq 0, \quad \eta = 0 \text{ when } \mathbf{B} = \mathbf{I}, \quad K = 3, \quad \eta \sim K \to \infty \text{ as } K \to \infty,$$
$$(4.12)$$

and the choice of orthotropic invariants ξ_r implies, for each r,

$$\xi \to -\infty \text{ as } b \to 0, \quad \xi = 0 \text{ at } b = 1, \quad \xi \to \infty \text{ as } b \to \infty, \quad (4.13)$$

so the ordering $(4.1)_3$ becomes

$$\xi_1 \geq \xi_2 \geq \xi_3. \quad (4.14)$$

The new features are the isotropic weighting factors $h(\eta)$, $\alpha(\eta)$, $c(\eta)$ and $\delta(\eta)$; the latter controlling the weight of the orthotropic terms. For (4.10) to become the instantaneous response (3.2) when $\mathbf{B} = \mathbf{I}$: $\eta = 0$, $\xi_1 = \xi_2 = \xi_3 = 0$, the weighting functions must have the limit values

$$\alpha(0) = 1, \quad c(0) = 0, \quad h(0) = 0, \quad g(0) = 0, \quad f(0) = 0, \quad (4.15)$$

with $\delta(0)$ determined by the limit of the function $\delta(\eta)$ obtained in the later correlations. The evolving anisotropy is due to the terms with response coefficients $f(\xi)$.

Note that $K \geq 3$ is necessary for real η, not confirmed in the earlier papers. By (4.2),

$$K = b_1 + b_2 + 1/(b_1 b_2), \quad \frac{\partial K}{\partial b_1} = 1 - 1/(b_1^2 b_2), \quad \frac{\partial K}{\partial b_2} = 1 - 1/(b_1 b_2^2),$$
$$(4.16)$$

which show that the only stationary point is at $b_1 = b_2 = b_3 = 1$ where $K = 3$, and this is a minimum by (4.12).

In a co-ordinate system with unit base vectors $\mathbf{e}^{(r)}$, $(r = 1,2,3)$, $\mathbf{B}$ is diagonal with components b_r, and the only non-zero component of each structure tensor $\mathbf{M}^{(r)}$ is the (rr) component, which is unity. For an applied single component shear strain-rate $\overline{D}_{rs}$, $(r \neq s)$ at this deformation, the constitutive relation (4.10) gives the instantaneous response

$$\hat{\sigma}_{rs} = \{\phi_1(0) + c(\eta) + [b_r + b_s]g(\eta) + \delta(\eta)[f(\xi_r) + f(\xi_s)]\}\overline{D}_{rs} = 2\mu_{rs}\overline{D}_{rs},$$
$$(4.17)$$

which defines the instantaneous directional viscosity μ_{rs}. Immediately (4.4) is satisfied, and also the equality $\mu_{13} = \mu_{23}$ in (4.5) with $b_1 = b_2$, $\xi_1 = \xi_2$, and the equality $\mu_{13} = \mu_{12}$ in (4.9) with $b_2 = b_3$, $\xi_2 = \xi_3$. However, the equality $\mu_{23} = \mu_{12}$ in (4.7), where $b_2 = 1$, $\xi_2 = 0$ requires

$$2(\mu_{23} = \mu_{12}) = g(\eta)[b_3 - b_1] + \delta(\eta)[f(\xi_3) - f(\xi_1)] = 0. \quad (4.18)$$

Now, with $b_2 = 1$, $b_3 = 1/b_1$, and hence

$$\xi_1 = b_1 - 1/b_1 = -\xi_3, \quad (K - 1)^2 = b_1^2 + 1/b_1^2 + 2 \to \eta^2 = (b_1 - 1/b_1)^2$$
$$= \xi_1^2, \quad (4.19)$$

(4.18) becomes

$$\eta g(\eta) = -2\delta(\eta)f^o(\eta), \quad f(\eta) = f^e(\eta) + f^o(\eta), \quad (4.20)$$

where $f^e(\eta)$ and $f^o(\eta)$ are the even and odd parts of f. This result was derived by Morland and Staroszczyk (2003) in the case $\delta(\eta) = 1$, when $g(\eta)$ is determined by $f(\eta)$ and is not an additional independent response coefficient.

With this relation for $g(\eta)$, we cannot determine analytically the conditions on $f(\eta)$ which ensure that the inequalities (4.5)–(4.9) are satisfied. Example correlations by Morland and Staroszczyk (2003) confirmed the inequalities numerically for those examples over a range of η. Instead, we now analyse a reduced form of (4.10) in which the $g(\eta)$ term is omitted; thus

$$f(0) = 0, \quad g(\eta) = 0, \quad f^o(\eta) = 0 \quad \to \quad f(\eta) \text{ is even.} \quad (4.21)$$

First suppose $\delta(\eta)$ is positive for all positive η; if negative then the sign of $f(\xi)$ is reversed in the following results. Now the inequalities (4.5)–(4.7) translate to

$$2[\mu_{12} - \mu_{23}] = \delta(\eta)[f(\xi_1) - f(\xi_3)] > 0, \quad 2[\mu_{23} - \mu_{13}]$$
$$= \delta(\eta)[f(\xi_2) - f(\xi_1)] > 0, \quad (4.22)$$

for $\xi_1 > \xi_2 > 0 > \xi_3$. Further, $b_3 b_1 = 1/b_2 < 1$ so $b_3 < 1/b_1$, and hence $-\xi_3 > \xi_1$. Fig. 2 illustrates the above relative positions ξ_1, ξ_2, ξ_3 shown over the curve marked f_1. Immediately, $f(\xi_1) < f(\xi_2)$ and $f(\xi_3) < f(\xi_1)$ are satisfied, and hence the inequalities (4.22), if and only if

$$f(\xi) < 0 \text{ and } f'(\xi) < 0 \text{ for all } \xi > 0 \to f'(\xi) > 0 \text{ for all } \xi < 0.$$
$$(4.23)$$

The inequalities (4.8) and (4.9) translate to

$$2[\mu_{23} - \mu_{12}] = \delta(\eta)[f(\xi_3) - f(\xi_1)] > 0, \quad 2[\mu_{12} - \mu_{13}]$$
$$= \delta(\eta)[f(\xi_2) - f(\xi_3)] > 0, \quad (4.24)$$

for $\xi_1 > 0 > \xi_2 > \xi_3$. Here $b_2 < 1$ so $b_3 > 1/b_1$ and hence $\xi_1 > -\xi_3$. The relative positions of ξ_1, ξ_2, ξ_3 are shown under the curve in Fig. 2 marked f_5. Immediately, $f(\xi_2) > f(\xi_3)$ and $f(\xi_3) > f(\xi_1)$ as required. In summary, validity of all the *Staroszczyk Equalities and Inequalities* is guaranteed by the function $f(\xi)$ having the properties (4.21) and (4.23). The shape of the function $f(\xi)$ is illustrated by two example curves marked f_1 and f_5 in Fig. 2. Note the large range of ξ which is required in the uni-axial compression analysis later. Recall that
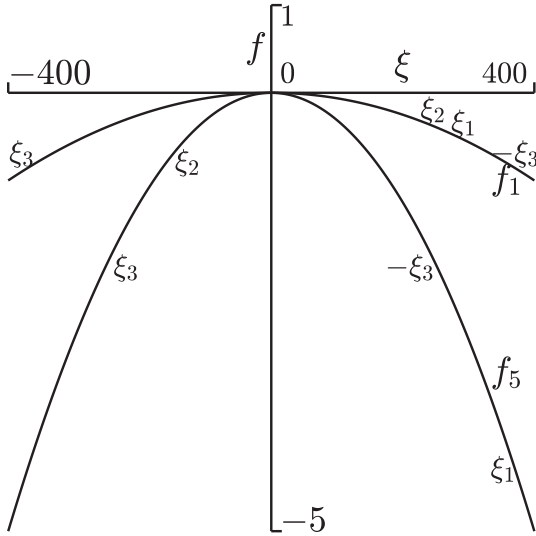
Fig. 2. Response coefficient $f(\xi)$.

$f(\eta)$ must change sign, and becomes positive if $\delta(\eta) < 0$ for all positive η.

It remains to show how the relation (4.10) allows correlation with families of laterally confined simple shear and uni-axial tertiary responses. Budd and Jacka (1989) and Li et al. (1996) have determined experimentally the limit ratios A and S respectively of fabric induced viscosity to initial isotropic viscosity for indefinite axial compression with equal unconfined lateral extensions, and for indefinite shear in a plane deformation. Mangeney et al. (1996) deduced values of A and S from the Greenland ice core data of Thorsteinsson et al. (1997). The reciprocals of these ratios, A^{-1} and S^{-1}, are described in the literature as enhancement factors. Simple shear and uni-axial compressive stress are basic one-dimensional tests and each can determine one response function of one invariant argument. Idealised families consistent with these properties will be adopted for illustration.

5. Laterally confined shear response

First consider a plane simple shear deformation from the isotropic state with shear strain κ and strain-rate $\dot{\gamma}$ at melt temperature, defined by

$$x_1 = X_1 + \kappa X_3, \quad x_2 = X_2, \quad x_3 = X_3, \quad \dot{\kappa} = 2\dot{\gamma} > 0, \quad \kappa \geq 0. \tag{5.1}$$

The corresponding deformation gradient $\mathbf{F}$, left Cauchy-Green tensor $\mathbf{B} = \mathbf{F}\mathbf{F}^T$, and deformation gradient rate $\dot{\mathbf{F}}$ are

$$\mathbf{F} = \begin{pmatrix} 1 & 0 & \kappa \\ 0 & 1 & 0 \\ 0 & 0 & 1 \end{pmatrix}, \quad \mathbf{B} = \begin{pmatrix} 1+\kappa^2 & 0 & \kappa \\ 0 & 1 & 0 \\ \kappa & 0 & 1 \end{pmatrix}, \quad \dot{\mathbf{F}} = \begin{pmatrix} 0 & 0 & \dot{\kappa} \\ 0 & 0 & 0 \\ 0 & 0 & 0 \end{pmatrix}. \tag{5.2}$$

The velocity field $\mathbf{v}$ has components

$$v_1 = \dot{\kappa}X_3, \quad v_2 = 0, \quad v_3 = 0, \tag{5.3}$$

so the only non-zero material and spatial velocity gradients are

$$\frac{\partial v_1}{\partial X_3} = \frac{\partial v_1}{\partial x_3} = \dot{\kappa}. \tag{5.4}$$

Hence, the spatial velocity gradient tensor $\mathbf{L}$ with symmetric part $\mathbf{D}$, the strain-rate tensor, and the shear strain-rate $\dot{\gamma}$, are

$$\mathbf{L} = \begin{pmatrix} 0 & 0 & \dot{\kappa} \\ 0 & 0 & 0 \\ 0 & 0 & 0 \end{pmatrix}, \quad \mathbf{D} = \frac{1}{2}[\mathbf{L} + \mathbf{L}^T] = \begin{pmatrix} 0 & 0 & \dot{\gamma} \\ 0 & 0 & 0 \\ \dot{\gamma} & 0 & 0 \end{pmatrix}, \quad \dot{\gamma} = \frac{1}{2}\dot{\kappa}. \tag{5.5}$$

Note that $(5.2)_3$ and $(5.5)_1$ confirm $\dot{\mathbf{F}} = \mathbf{LF}$. The corresponding deviatoric stress tensor $\hat{\sigma}$ is

$$\hat{\sigma} = \begin{pmatrix} \hat{\sigma}_{11} & 0 & \tau \\ 0 & \hat{\sigma}_{22} & 0 \\ \tau & 0 & \hat{\sigma}_{33} \end{pmatrix}, \tag{5.6}$$

where $\hat{\sigma}_{11}, \hat{\sigma}_{22}, \hat{\sigma}_{33}$ are constraint stresses necessary to maintain the plane shear deformation, with trace$(\hat{\sigma}) = \hat{\sigma}_{11} + \hat{\sigma}_{22} + \hat{\sigma}_{33} = 0$, and $\tau = \hat{\sigma}_{13}$.[3]

The principal stretch squares b_i ($i = 1,2,3$), the eigenvalues of $\mathbf{B}$ determined from (4.1), the associated principal vectors $\mathbf{e}^{(r)}$ and the strain-rate invariant are given by

$$b_2 = 1, \quad b_3 = b_1^{-1}, \quad 2b_1 = 2 + \kappa^2 + \sqrt{(2+\kappa^2)^2 - 4}, \quad \bar{I} = \dot{\gamma}^2, \tag{5.7}$$

$$\mathbf{e}^{(2)} = (0,1,0), \quad e_2^{(s)} = 0, \quad \kappa e_1^{(s)} + (1-b_s)e_3^{(s)} = 0,$$
$$[e_1^{(s)}]^2 + [e_3^{(s)}]^2 = 1 \quad (s = 1,3). \tag{5.8}$$

The three orthotropic structure tensors, defined by equation $(4.11)_1$, are

$$\mathbf{M}^{(2)} = \begin{pmatrix} 0 & 0 & 0 \\ 0 & 1 & 0 \\ 0 & 0 & 0 \end{pmatrix}, \quad \mathbf{M}^{(s)} = \begin{pmatrix} e_1^{(s)}e_1^{(s)} & 0 & e_1^{(s)}e_3^{(s)} \\ 0 & 0 & 0 \\ e_1^{(s)}e_3^{(s)} & 0 & e_3^{(s)}e_3^{(s)} \end{pmatrix} \quad (s = 1,3), \tag{5.9}$$

and the fabric response coefficient arguments, given by $(4.11)_2$ and $(4.11)_3$, are

$$\xi_1 = -\xi_3 = \eta = \sqrt{(2+\kappa^2)^2 - 4}, \quad \xi_2 = 0. \tag{5.10}$$

Note that $\mathbf{D}^2$ is a diagonal tensor with two non-trivial components (11) and (33) both equal to $\dot{\gamma}^2$; that is, it has zero (13)-component which means that $\mathbf{D}^2$ has no effect on the shear response of ice.

The flow law (4.10) with $g(\eta) = 0$ gives relations for the two independent diagonal constraint stress components, together with the shear relation for the required shear stress τ:

$$\tau = \alpha(\eta)\phi_1(\dot{\gamma}^2)\dot{\gamma} + \beta(\eta)\dot{\gamma} = \alpha(\eta)V_s(\dot{\gamma}) + \beta(\eta)\dot{\gamma},$$
$$\beta(\eta) = c(\eta) + 2\delta(\eta)f(\eta), \tag{5.11}$$

involving only the combination $\beta(\eta)$ of $c(\eta)$ and $\delta(\eta)f(\eta)$, and independent of $h(\eta)$. Here $V_s(\dot{\gamma})$ is the initial viscous shear response given by

$$V_s(\dot{\gamma}) = \phi_1(\dot{\gamma}^2)\dot{\gamma}, \quad \tau = V_s(\dot{\gamma}_I), \tag{5.12}$$

independent of $\phi_2(\bar{I})$, with the qualitative behaviour shown in Fig. 3. τ is determined uniquely in terms of the initial strain-rate $\dot{\gamma}_I$ by the instantaneous viscous response. Hence, for each constant τ, constant $\dot{\gamma}_I$,

$$\beta(\eta)\dot{\gamma} + \alpha(\eta)V_s(\dot{\gamma}) = V_s(\dot{\gamma}_I). \tag{5.13}$$

Given the response coefficients $\beta(\eta)$, and weighting coefficient $\alpha(\eta)$ independent of $f(\eta)$, (5.13) is an implicit equation for the tertiary creep family $\dot{\gamma} = \omega(\eta, \dot{\gamma}_I)$.

Alternatively, given the tertiary creep family $\dot{\gamma} = \omega(\eta, \dot{\gamma}_I)$, where, from the observed shapes of tertiary responses illustrated in Fig. 4 by the continuous curves,

$$\omega(0, \dot{\gamma}_I) = \dot{\gamma}_I, \quad \frac{\partial\omega}{\partial\eta} < 0, \quad \frac{\partial\omega}{\partial\dot{\gamma}_I} > 0, \tag{5.14}$$

(5.13) determines a different combination of $\beta(\eta)$ and $\alpha(\eta)$ for each $\dot{\gamma}_I$. That is, the law (4.10) is not sufficiently general to allow arbitrary prescribed tertiary creep responses at more than two constant shear stresses. However, given a family of tertiary responses at different shear stresses, we can choose that for the minimum stress τ_m with initial strain-rate $\dot{\gamma}_m$, and that for the maximum stress τ_x with initial strain-rate $\dot{\gamma}_x$, to determine $\alpha(\eta)$ and $\beta(\eta)$ from the two simultaneous equations

---

[3] A simple shear stress with $\hat{\sigma}_{11} = \hat{\sigma}_{22} = \hat{\sigma}_{33} = 0$ requires axial strain-rate components and a more complicated analysis involving difference relations.
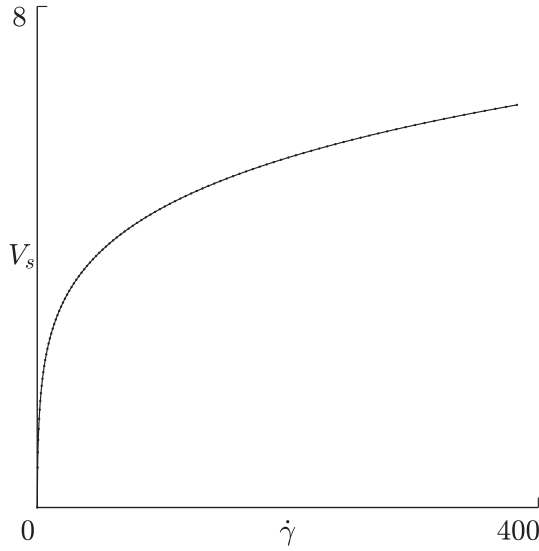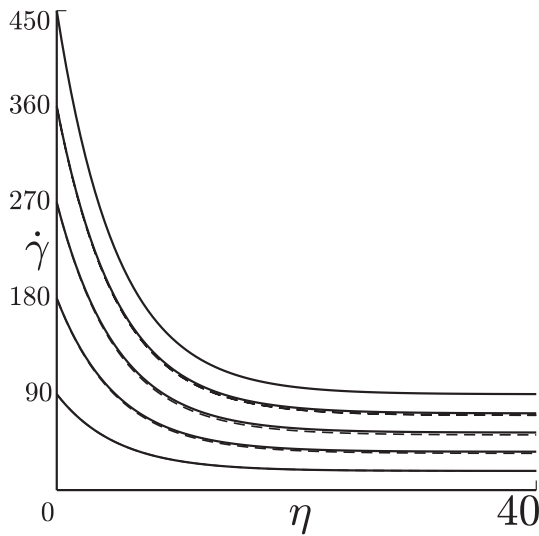
Fig. 3. Initial viscous response in shear.

Fig. 4. Tertiary creep curves for shear; continuous lines assumed family, dashed lines predicted by model.

$$\omega(\eta, \dot{\gamma}_m)\beta(\eta) + V_s[\omega(\eta, \dot{\gamma}_m)]\alpha(\eta) = \tau_m = V_s(\dot{\gamma}_m), \tag{5.15}$$

$$\omega(\eta, \dot{\gamma}_x)\beta(\eta) + V_s[\omega(\eta, \dot{\gamma}_x)]\alpha(\eta) = \tau_x = V_s(\dot{\gamma}_x). \tag{5.16}$$

It is anticipated that the predicted tertiary responses for the interim stresses with these coefficients will be of similar shape and lie between the two limit responses.

The unique solution for each positive η is

$$[\omega_m V_s(\omega_x) - \omega_x V_s(\omega_m)]\beta(\eta) = V_s(\dot{\gamma}_m)V_s(\omega_x) - V_s(\dot{\gamma}_x)V_s(\omega_m), \tag{5.17}$$

$$[\omega_m V_s(\omega_x) - \omega_x V_s(\omega_m)]\alpha(\eta) = \omega_m V_s(\dot{\gamma}_x) - \omega_x V_s(\dot{\gamma}_m), \tag{5.18}$$

where

$$\omega_m = \omega(\eta, \dot{\gamma}_m), \quad \omega_x = \omega(\eta, \dot{\gamma}_x). \tag{5.19}$$

Immediately, by $(5.14)_1$, $\beta(0) = 0$ and $\alpha(0) = 1$. The common LHS [·] of (5.17) and (5.18), for fixed ω_m, is

$$L(\omega_x) = \omega_m V_s(\omega_x) - \omega_x V_s(\omega_m), \quad L'(\omega_x) = \omega_m V_s'(\omega_x) - V_s(\omega_x), \tag{5.20}$$

with $L(\omega_m) = 0$. Now the positive gradient of $V_s(\dot{\gamma})$ is decreasing, so $V_s(\omega_x) = V_s'(\omega_x)[\omega_x + d]$ for some positive d, and hence

$$L'(\omega_x) = \omega_m V_s'(\omega_x) - V_s'(\omega_x)[\omega_x + d]$$
$$= -V_s'(\omega_x)[\omega_x - \omega_m + d] < 0 \quad \rightarrow \quad L(\omega_x) < 0. \tag{5.21}$$

Now (5.18) re-arranges to

$$L(\omega_x)[\alpha(\eta) - 1] = [\omega_x - \omega_m]\{V_s(\omega_x) - V_s(\dot{\gamma}_x)\} < 0, \tag{5.22}$$

since RHS [·] > 0 and RHS {·} < 0, and hence $\alpha(\eta) > 1$ for $\eta > 0$. We have not determined any such result for $\beta(\eta)$. Note that shear correlation does not depend on a prescribed $f(\eta)$.

6. Uni-axial compression response

Next consider uni-axial compression along the Ox_3 axis with compressive stress $\sigma > 0$, axial stretch $b_3 < 1$ and compressive axial strain-rate $\dot{\epsilon} > 0$, described by

$$\mathbf{B} = \begin{pmatrix} b_1 & 0 & 0 \\ 0 & b_1 & 0 \\ 0 & 0 & b_3 \end{pmatrix}, \quad \mathbf{D} = \begin{pmatrix} d_1 & 0 & 0 \\ 0 & d_1 & 0 \\ 0 & 0 & -\dot{\epsilon} \end{pmatrix}, \quad \sigma = \begin{pmatrix} 0 & 0 & 0 \\ 0 & 0 & 0 \\ 0 & 0 & -\sigma \end{pmatrix}. \tag{6.1}$$

Due to the ice incompressibility conditions det$\mathbf{B} = 1$ and trace $(\mathbf{D}) = 0$ we have $b_1^2 b_3 = 1$ and $2d_1 = \dot{\epsilon}$. By (3.1), non-zero deviatoric stress tensor components are $\hat{\sigma}_{11} = \hat{\sigma}_{22} = \frac{1}{3}\sigma$ and $\hat{\sigma}_{33} = -\frac{2}{3}\sigma$. The three principal unit vectors $\mathbf{e}^{(r)}$ defining the orthotropic symmetries of the material are now $\mathbf{e}^{(1)} = (1,0,0)$, $\mathbf{e}^{(2)} = (0,1,0)$ and $\mathbf{e}^{(3)} = (0,0,1)$, so that the structure tensors $\mathbf{M}^{(r)}$ defined by $(4.11)_1$ are given by

$$\mathbf{M}^{(1)} = \begin{pmatrix} 1 & 0 & 0 \\ 0 & 0 & 0 \\ 0 & 0 & 0 \end{pmatrix}, \quad \mathbf{M}^{(2)} = \begin{pmatrix} 0 & 0 & 0 \\ 0 & 1 & 0 \\ 0 & 0 & 0 \end{pmatrix}, \quad \mathbf{M}^{(3)} = \begin{pmatrix} 0 & 0 & 0 \\ 0 & 0 & 0 \\ 0 & 0 & 1 \end{pmatrix}. \tag{6.2}$$

Further, the three orthotropic invariants ζ_r, defined by $(4.11)_2$, are

$$\xi_1 = \xi_2 = b_1 - b_1^{-1} = b_3^{-\frac{1}{2}} - b_3^{\frac{1}{2}} \geq 0, \quad \xi_3 = b_1^{-2} - b_1^2 = b_3 - b_3^{-1} \leq 0, \tag{6.3}$$

and the isotropic invariant η, see $(4.11)_3$, is given by

$$\eta = [(2b_1 + b_1^{-2} - 1)^2 - 4]^{\frac{1}{2}} = \left[\left(2b_3^{-\frac{1}{2}} + b_3 - 1\right)^2 - 4\right]^{\frac{1}{2}} \geq 0. \tag{6.4}$$

It follows that both ξ_1 and η increase from zero as b_1 increases from unity (b_3 decreases from unity). The relation (6.4) can be inverted to express b_3 as a function $b_3(\eta)$, and hence the relations (6.3) determine ξ_1 and ξ_3 as functions $\xi_1(\eta)$ and $\xi_3(\eta)$. Fig. 5 shows the variation of b_1, b_3, ξ_1 and $-\xi_3/10$ with η, with ξ_3 scaled because of its large negative value for practical magnitudes of b_1 and η. Note that at $b_1 = 10$ the

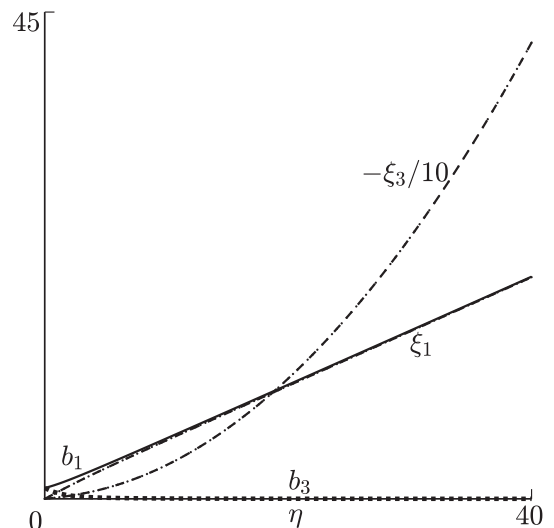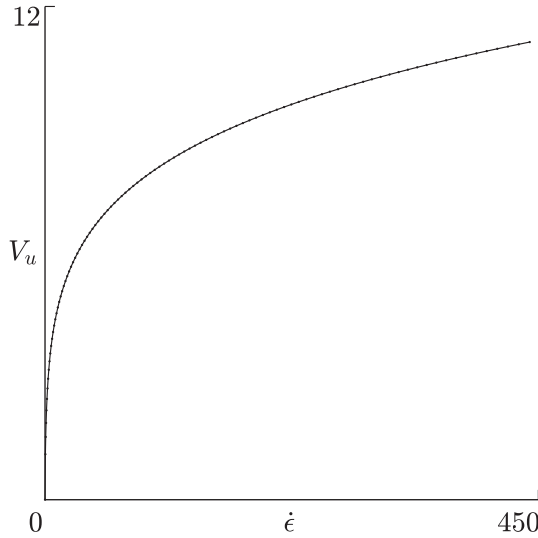**Fig. 5.** Deformation invariants in uni-axial compression.
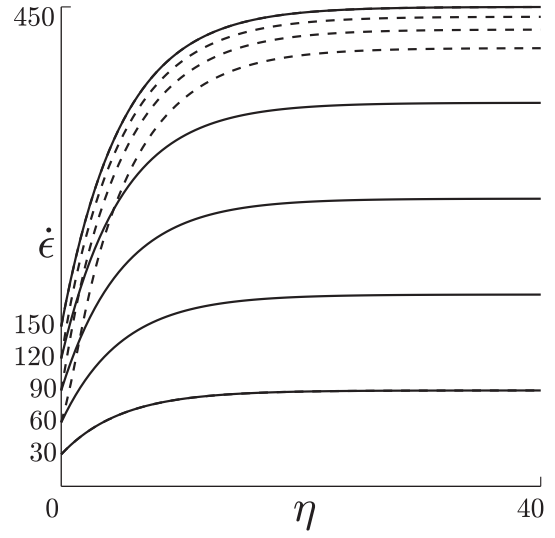
Fig. 6. Initial viscous response in uni-axial compression.

Fig. 7. Tertiary creep curves for uni-axial compression; continuous lines assumed family, dashed lines predicted by model.

compression is $b_3 = 0.01$.

The orthotropic flow law (4.10) gives the one independent relation

$$\sigma = \alpha(\eta)V_u(\dot\varepsilon) - \frac{3}{4}h(\eta)\dot\varepsilon^2 + \left[\frac{3}{2}c(\eta) + \delta(\eta)\{f(\xi_1) + 2f(\xi_3)\}\right]\dot\varepsilon,$$

$$V_u(\dot\varepsilon) = \frac{3}{2}\phi_1(\bar I)\dot\varepsilon - \frac{3}{4}\phi_2(\bar I)\dot\varepsilon^2, \tag{6.5}$$

where $V_u(\dot\varepsilon)$ is the initial viscous response with qualitative behaviour shown in Fig. 6. When the stress σ is applied, there is an initial viscous response strain-rate $\dot\varepsilon_I$ given by

$$\sigma = V_u(\dot\varepsilon_I) = \frac{3}{2}\phi_1(\bar I_I)\dot\varepsilon_I - \frac{3}{4}\phi_2(\bar I_I)\dot\varepsilon_I^2, \quad \bar I_I = \frac{3}{4}\dot\varepsilon_I^2. \tag{6.6}$$

Then, for each constant σ, equivalently constant initial strain-rate $\dot\varepsilon_I$, (6.5) becomes

$$\alpha(\eta)V_u(\dot\varepsilon) - \frac{3}{4}h(\eta)\dot\varepsilon^2 + \left[\frac{3}{2}c(\eta) + \delta(\eta)\{f(\xi_1) + 2f(\xi_3)\}\right]\dot\varepsilon = V_u(\dot\varepsilon_I). \tag{6.7}$$

Given all the response coefficients and weighting factors, this is an implicit equation for the subsequent family of tertiary creep curves $\dot\varepsilon = \chi(\eta, \dot\varepsilon_I)$ for different initial strain-rates, which have the properties

$$\chi(0, \dot\varepsilon_I) = \dot\varepsilon_I, \quad \frac{\partial\chi}{\partial\eta} > 0, \quad \frac{\partial\chi}{\partial\dot\varepsilon_I} > 0, \tag{6.8}$$

illustrated in Fig. 7.

Alternatively, rearranging (6.7) and substituting for $c(\eta)$ in terms of $\beta(\eta)$ and $f(\eta)$, yields

$$h(\eta)\dot\varepsilon^2 + \delta(\eta)\left\{4f(\eta) - \frac{4}{3}f(\xi_1) - \frac{8}{3}f(\xi_3)\right\}\dot\varepsilon$$

$$= \frac{4}{3}\alpha(\eta)V_u(\dot\varepsilon) - \frac{4}{3}V_u(\dot\varepsilon_I) + 2\beta(\eta)\dot\varepsilon, \tag{6.9}$$

where $\alpha(\eta)$ and $\beta(\eta)$ have been determined by the shear response. Eq. (6.9) expresses a combination of $h(\eta)$, $\delta(\eta)$ and $f(\xi)$ in terms of the known RHS, but involving $f(\xi)$ at three different ξ. That is, (6.9) provides a difference relation for $f(\xi)$, not an explicit algebraic relation. While the shear relation (5.13) only involves the combination $\beta(\eta)$, not requiring a prescribed $f(\xi)$, (6.9) requires a prescribed $f(\xi)$ to become an algebraic relation for $h(\eta)$, and $\delta(\eta)$. With the prescription of a family of $f(\xi)$ which satisfies the SEI validity conditions, illustrated in Fig. 2, (6.9) can be applied at two values of $\dot\varepsilon_I$ to provide two simultaneous equations for $h(\eta)$ and $\delta(\eta)$. As with the shear analysis, we choose a minimum strain-rate $\dot\varepsilon_I = \dot\varepsilon_m$ and maximum strain-rate $\dot\varepsilon_I = \dot\varepsilon_x$,

anticipating that the resulting interim tertiary response curves will be monotonic and lie between the correlated outer curves.

Recall that (6.3) and (6.4) determine ξ_1 and ξ_3 as functions of η, so we can define the combination

$$F(\eta) = 4f(\eta) - \frac{4}{3}f(\xi_1) - \frac{8}{3}f(\xi_3). \tag{6.10}$$

Next we define the combination

$$V(\chi(\eta), \dot\varepsilon_I) = \frac{4}{3}[\alpha(\eta)V_u(\chi) - V_u(\dot\varepsilon_I)], \tag{6.11}$$

where

$$\dot\varepsilon = \chi(\eta, \dot\varepsilon_I), \quad \chi_m = \chi(\eta, \dot\varepsilon_m), \quad \chi_x = \chi(\eta, \dot\varepsilon_x), \tag{6.12}$$

and $V(0, \dot\varepsilon_I) = 0$, and $F(0) = 0$ for any $f(0)$. The simultaneous equations are now

$$\chi_m^2 h(\eta) + \chi_m F(\eta)\delta(\eta) = V(\chi_m, \dot\varepsilon_m) + 2\beta(\eta)\chi_m,$$

$$\chi_x^2 h(\eta) + \chi_x F(\eta)\delta(\eta) = V(\chi_x, \dot\varepsilon_x) + 2\beta(\eta)\chi_x. \tag{6.13}$$

These have the unique solution for each positive η:

$$\chi_x\chi_m(\chi_x - \chi_m)h(\eta) = -\chi_x V(\chi_m, \dot\varepsilon_m) + \chi_m V(\chi_x, \dot\varepsilon_x),$$

$$\chi_x\chi_m(\chi_x - \chi_m)F(\eta)\delta(\eta)$$

$$= \chi_x^2 V(\chi_m, \dot\varepsilon_m) - \chi_m^2 V(\chi_x, \dot\varepsilon_x) + 2\chi_x\chi_m(\chi_x - \chi_m)\beta(\eta), \tag{6.14}$$

which show h is independent of $f(\eta)$ and $h(0) = 0$, but that $\delta(0)$ is indeterminate and must be determined by a limit process. Given a smooth even $f(\eta)$ with $f(0) = 0$, then $f(\eta) \sim -k\eta^2$, or smaller. Setting $b_1 = 1 + \varepsilon$ and letting $\varepsilon \to 0$, then $\xi_1 \sim 2\varepsilon$, $\xi_3 \sim -4\varepsilon$, $\eta \sim 2\left(3\frac{1}{2}\right)\varepsilon$. Hence $f(\xi_1) \sim \frac{1}{3}f(\eta)$ and $f(\xi_3) \sim \frac{4}{3}f(\eta)$, so $F(\eta) \sim -k\eta^2\left[4 - \frac{4}{3}\frac{1}{3} - \frac{8}{3}\frac{4}{3}\right]$ where $[\cdot] = 0$. Thus $F(\eta)$ is smaller than $f(\eta)$, probably $O(\eta)f(\eta)$, and hence the expression (6.14)$_2$ for $\delta(\eta)$ is indeterminate at $\eta = 0$ and $\delta(\eta) \to \infty$. However, $\delta(\eta)F(\eta)$ given by (6.14)$_2$ is bounded. In the current shear deformation, $\delta(\eta)$ only arises in the combinations $\delta(\eta)f(\eta)$, $\delta(\eta)f(\xi_1)$ and $\delta(\eta)f(\xi_3)$, which can be determined from $\delta(\eta)F(\eta)$, and are bounded. Given $f(\eta)$, then

$$f(\xi_1) = s_1(\eta)f(\eta), \quad f(\xi_3) = s_3(\eta)f(\eta), \tag{6.15}$$

where the ratios $s_1(\eta)$ and $s_3(\eta)$ follow from the known $\xi_1(\eta)$ and $\xi_3(\eta)$. Hence

$$\delta(\eta)f(\eta) = \delta(\eta)F(\eta)/[4 - 4s_1(\eta)/3 - 8s_3(\eta)/3], \tag{6.16}$$

still with the indeterminancy at $\eta = 0$ to be completed by a limit process, constructing a quadratic representation which passes through the next three points. $f(\xi_1)$ and $f(\xi_3)$ then follow from (6.15).

Recall that a valid solution requires $\delta(\eta) > 0$, which we have not been able to show analytically from (6.14)$_2$. Given the response coefficients $f(\eta)$, $f(\xi_1)$, $f(\xi_3)$, $\beta(\eta)$, $h(\eta)$ and weighting coefficient $\alpha(\eta)$, (6.9) is an implicit equation for the tertiary creep family $\dot{\varepsilon} = \chi(\eta, \dot{\varepsilon}_I)$ corresponding to different initial strain-rates $\dot{\varepsilon}_I$.

A similar analysis applies to a general deformation with three evolving distinct orthotropic invariants ξ_1, ξ_2, ξ_3.

7. Correlation with prescribed tertiary creep responses

Tertiary creep can be described in terms of "strain-rate enhancement" with the decompositions

$$\omega(\eta_s, \dot{\gamma}_I) = \dot{\gamma}_I S(\eta_s, \dot{\gamma}_I), \quad \chi(\eta, \dot{\varepsilon}_I) = \dot{\varepsilon}_I A(\eta, \dot{\varepsilon}_I), \tag{7.1}$$

for the shear and uni-axial responses, respectively, where $\overline{S}(\dot{\gamma}_I) = S(\infty, \dot{\gamma}_I)$ and $\overline{A}(\dot{\varepsilon}_I) = A(\infty, \dot{\varepsilon}_I)$ are the reciprocals of the shear and uni-axial enhancement factors. These have the properties

$$S(0, \dot{\gamma}_I) = \dot{\gamma}_I; \quad \text{and as} \quad \eta \to \infty: \dot{\gamma} \to \dot{\gamma}_T = \dot{\gamma}_I \overline{S}(\dot{\gamma}_I), \quad \overline{S}(\dot{\gamma}_I) < 1, \tag{7.2}$$

$$A(0, \dot{\varepsilon}_I) = \dot{\varepsilon}_I; \quad \text{and as} \quad \eta \to \infty: \dot{\varepsilon} \to \dot{\varepsilon}_T = \dot{\varepsilon}_I \overline{A}(\dot{\varepsilon}_I), \quad \overline{A}(\dot{\varepsilon}_I) > 1. \tag{7.3}$$

It is commonly assumed that the ratio $\overline{S}$ is constant, less than unity, and $\overline{S} = 0.2$ has been proposed. Similarly, $\overline{A}$ is assumed constant with the proposed value $\overline{A} = 3$. These idealisations are now adopted for our illustrations, with $S(\eta)$ decreasing monotonically from unity to $\overline{S}$ and $A(\eta)$ increasing monotonically from unity to $\overline{A}$, thus

$$S(\eta) = 1 - (1 - \overline{S})[1 - \exp(-s\eta)],$$
$$A(\eta) = 1 + (\overline{A} - 1)[1 - \exp(-a\eta)], \tag{7.4}$$

where the parameters s and a define how quickly the limit values are reached. One value of each is chosen, $s = 0.2$ and $a = 0.2$, as examples to show the expected qualitative behaviour of the respective families of tertiary creep for a range of initial strain-rates $\dot{\gamma}_I$ and $\dot{\varepsilon}_I$, shown in Figs. 4 and 7, respectively.

Fig. 8 shows the deduced constitutive coefficients $\beta(\eta)$ and $\alpha(\eta)$ for $s = 0.2$ from the shear results (5.18), (5.19) and (7.4) based on the minimum and maximum initial strain-rates of the family $\dot{\gamma}$: $\dot{\gamma}_I = 90, 180, 270, 360, 450$. Note that the figure shows $\beta(\eta)$ scaled by 100, since β remains close to zero to balance the large strain-rates in the present variables. An approximation $\beta = 0$ would not allow the correlations at two values of $\dot{\gamma}_I$. Here $\alpha(\eta)$ increases monotonically from
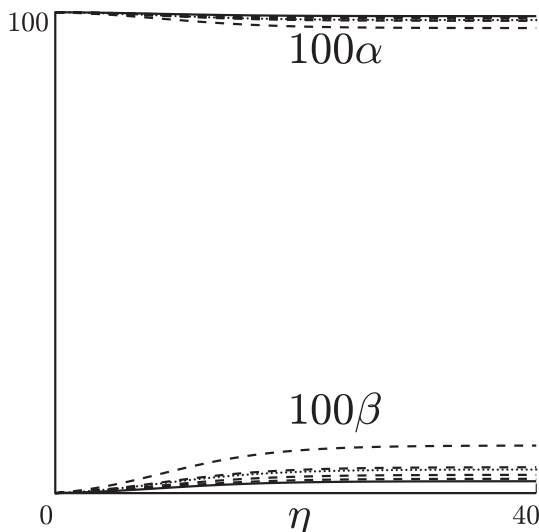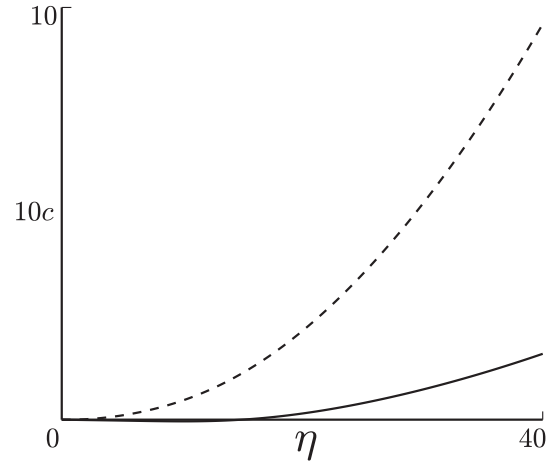

Fig. 9. Response coefficients $c(\eta)$ for $f_c = 1$, solid line, and $f_c = 5$, dashed line.

unity, and $\beta(\eta)$ decreases monotonically from zero, as η increases from zero.

We consider two orthotropic response coefficients $f(\xi)$ which satisfy the *SEI*, illustrated in Fig. 2, namely

$$f(\xi) = -f_c \xi^2 / \xi_{\max}^2, \quad f_c = f_1, \ f_5, \quad \xi_{\max} = 400, \tag{7.5}$$

with two parameters $f_1 = 1$ and $f_5 = 5$ as examples, which then determine the corresponding $c(\eta)$ from $\beta(\eta)$ illustrated in Fig. 9. The continuous curve is for $f_c = 1$ and the dashed curve for $f_c = 5$; note the scaling of c by a factor 10. However, it is convenient to replace $c(\eta)$ in terms of $\beta(\eta)$ and $f(\eta)$ for application to the uni-axial response from which $h(\eta)$ and $\delta(\eta)f(\eta)$ are given by (6.14). The resulting $h(\eta)$ is independent of $f(\eta)$ and is extremely small, to balance the large strain-rates squared in the present variables. It is shown scaled by 10^4 in Fig. 10. With this $f(\xi)$ it follows immediately from (6.15) that

$$s_1(\eta) = \xi_1^2(\eta)/\eta^2, \quad s_3(\eta) = \xi_3^2(\eta)/\eta^2, \tag{7.6}$$

and (6.16) becomes

$$\delta(\eta)f(\eta) = \delta(\eta)F(\eta)/D, \quad D = 4 - \frac{4\xi_1^2}{3\eta^2} - \frac{8\xi_3^2}{3\eta^2}. \tag{7.7}$$

The indeterminancy at $\eta = 0$ is evaluated by a quadratic expansion obtained by matching the values at the three points beyond $\eta = 0$. The resulting $\delta(\eta)F(\eta)$ is also shown in Fig. 10, scaled by 10. The response coefficients $\delta(\eta)f(\eta)$, $\delta(\eta)\xi_1(\eta)$ and $\delta(\eta)\xi_3(eta)$, each scaled by 10, are shown in Fig. 11, independent of $f(\eta)$ for the assumed family (7.5).
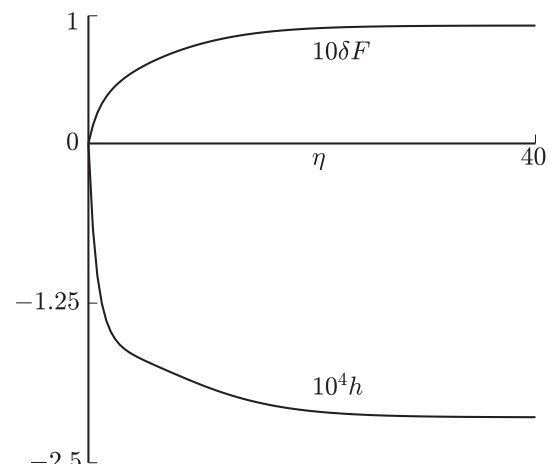

Fig. 8. Response coefficients $\alpha(\eta)$ and $\beta(\eta)$.

Fig. 10. Response coefficients $10^4 h(\eta)$ and $10\delta(\eta)F(\eta)$.
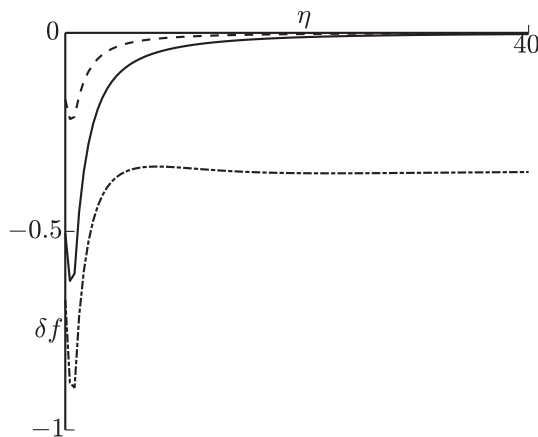
Fig. 11. Response coefficients $\delta(\eta)f(\eta)$, continuous line, $\delta(\eta)f[\xi_1(\eta)]$, dashed line, $\delta(\eta)f[\xi_3(\eta)]$, dash-dot line, each scaled by 10.

Importantly, we see that $\delta(\eta)f(\eta)$ is everywhere negative as required to ensure validity of the *SEI*, that is, $\delta(\eta)$ is positive for the adopted $f(\eta)$. $\delta(\eta)$ is then given by (7.7) for a given $f(\eta)$, but is unbounded at $\eta = 0$. However, $\delta(\eta)$ only arises in a combination

$$\delta(\eta)f(\xi(\eta)) = \delta(\eta)f(\eta)[f(\xi(\eta)/f(\eta)], \tag{7.8}$$

where the [·] fraction is determined by the adopted $f(\eta)$ for a required $\xi(\eta)$. We now see for this choice of the $f(\xi)$ family that the response coefficients are independent of the parameter f_c, as are the implicit equations which determine the predicted responses for given initial shear and uni-axial strain-rates. However, the responses for different initial stress, strain-rate geometry will depend explicitly on $c(\eta)$, hence on f_c. Here we are only evaluating the particular shear and uni-axial compression response for comparison with the assumed tertiary creep families, to show the good correlations. Solution of the implicit eqs. (5.13) and (6.9) determine the predicted responses, automatically identical with the assumed curves at minimum and maximum initial strain-rates. Note that the interim assumed curves are not necessarily associated with the family of responses based on the minimum and maximum initial strain-rates, so close correlation is not essential. However, it is significant that the resulting responses have similar monotonic shapes lying within the envelopes defined by the minimum and maximum initial strain-rates.

Fig. 4 is the tertiary shear comparison, the assumed response shown as continuous lines and the model response shown as dashed lines. The curves for the minimum and maximum initial strain-rates are identical by the correlation. The comparisons at the interim initial strain-rates are surprisingly good, but the significant, validating, feature is that the interim curves are monotonic and lie within the envelope.

Fig. 7 is the uni-axial stress comparison, the assumed response shown as continuous lines and the model response shown as dashed lines. The curves for the minimum and maximum initial strain-rates are identical. The comparisons at the interim initial strain-rates have the significant, validating, feature that the interim curves are monotonic and lie within the envelope.

8. Conclusions

We have examined a subset of fabric evolution laws with orthotropic symmetry based on crystal rotation arguments, firstly to determine conditions which ensure that the *SEI* validity conditions on the directional viscosities are satisfied, and secondly to investigate how they can be approximately correlated with idealised laterally confined tertiary creep in simple shear, and in uni-axial compressive stress. It is shown that uni-axial stress response leads to difference relations in the correlation, not explicit relations. The uni-axial difference relations can

only be satisfied by adopting a family of orthotropic response coefficients, which satisfies the *SEI* validity conditions, and then determine the remaining response coefficients by correlations with tertiary creep curves for minimum and maximum initial strain-rates.

This is illustrated for an assumed family of orthotropic functions which ensure the *SEI* are satisfied. For the purpose of illustration it was supposed that the initial viscous response was described by the customary co-axial relation based on Glen's (1955) data from uni-axial stress experiments, for which the strain-rate formulation was correlated accurately by Smith and Morland (1981), and here an accurate equivalent for the stress formulation was derived.

An accurate constitutive relation requires first: accurate uni-axial and shear initial viscous data to determine the initial viscous response, which will require a quadratic relation, not the customary co-axial relation with one response coefficient; second: accurate families of tertiary creep data for shear deformation and uni-axial compression with different initial strain-rates, to determine the response coefficients in the orthotropic non-simple fluid law by correlation at the minimum and maximum initial strain-rates. But note that different shear and axial stress configurations can present explicit relations and difference relations for the correlations, so the choice of experimental configurations should reflect what is required.

Both the initial viscous response and tertiary creep response imply a very different constitutive law from the customary co-axial simple viscous fluid relation. The latter is the common assumption in the large-scale numerical codes used to compute ice-sheet flows in climate modelling, and must lead to significant differences from solutions using the non-simple fluid law described above. A steady radially symmetric flow example has already demonstrated such a difference (Morland and Staroszczyk, 2006). While the current simple viscous fluid law leads to a system of parabolic differential equations, the proposed non-simple fluid law leads to a much more numerically difficult system of mixed parabolic and hyperbolic differential equations which require very different numerical algorithms, not a modification of the present codes.

Declaration of Competing Interest

The authors declare that they have no known competing financial interests or personal relationships that could have appeared to influence the work reported in this paper.

Acknowledgement

References

Boehler, J., 1987. Representations for isotropic and anisotropic non-polynomial tensor functions. In: Boehler, J. (Ed.), Applications of Tensor Functions in Solid Mechanics. Springer, Berlin, pp. 31–53.
Budd, W., Jacka, T.H., 1989. A review of ice rheology for ice sheet modelling. Cold Reg. Sci. Technol. 16, 107–144.
Budd, W., Warner, R.C., Jacka, T.H., Li, J., Treverrow, A., 2013. Ice flow relations for stress and strain-rate components from combined shear and compression laboratory experiments. J. Glaciol. 59 (214), 374–392.
Faria, S.H., 2006. Creep and recrystallization of large polycrystalline masses. III. Continuum theory of ice sheets. Proc. R. Soc. Lond. A 462 (2073), 2797–2816. https://doi.org/10.1098/rspa.2006.1698.
Faria, S.H., Kremer, G.M., Hutter, K., 2003. On the inclusion of recrystallization processes in the modeling of induced anisotropy in ice sheeets: a thermodynamicist's point of view. Ann. Glaciol. 37, 29–34.
Gagliardini, O., Meyssonnier, J., 1999. Analytical derivations for the behavior and fabric evolution of a linear orthotropic ice polycrystal. J. Geophys. Res. 104 (B8), 17,797–17,809. https://doi.org/10.1029/1999JB900146.
Glen, J., 1955. The creep of polycrystalline ice. Proc. R. Soc. Lond. A 228, 519–538.
Gödert, G., Hutter, K., 1998. Induced anisotropy in large ice shields: theory and its

homogenization. Continuum Mech. Thermodyn. 10 (5), 293–318.

Li, J., Jacka, T.H., Budd, W., 1996. Deformation rates in combined compression and shear for ice which is initially isotropic and after the development of strong anisotropy. Ann. Glaciol. 23, 247–252.

Mangeney, A., Califano, F., Castelnau, O., 1996. Isothermal flow of an anisotropic ice sheet in the vicinity of an ice divide. J. Geophys. Res. 101, 189–204.

Mellor, M., Testa, R., 1969. Effect of temperature on the creep of ice. J. Glaciol. 8, 131–145.

Meyssonnier, J., Philip, A., 1996. A model for tangent viscous behaviour of anisotropic polar ice. Ann. Glaciol. 23, 253–261.

Morland, L.W., Lee, E.H., 1960. Stress analysis for linear viscoelastic materials with temperature variation. Trans. Soc. Rheol. 4, 233–263.

Morland, L.W., Spring, U., 1981. Viscoelastic uid relation for the deformation of ice. Cold Reg. Sci. Technol. 4, 255–268.

Morland, L.W., Staroszczyk, R., 1998. Viscous response of polar ice with evolving fabric. Contin. Mech. Thermodyn. 10, 135–152.

Morland, L.W., Staroszczyk, R., 2003. Stress and strain-rate formulations for fabric evolution in polar ice. Contin. Mech. Thermodyn. 15, 55–71.

Morland, L.W., Staroszczyk, R., 2006. Steady radial ice sheet flow with fabric evolution. J. Glaciol. 52, 267–280.

Morland, L.W., Staroszczyk, R., 2009. Viscosity enhancement in uni-axial compression and simple shear due to ice crystal rotation. Int. J. Eng. Sci. 47, 1297–1304.

Morland, L.W., Staroszczyk, R., 2019. The viscous relation for the initial isotropic response of ice. Cold Reg. Sci. Technol. 162, 11–18. https://doi.org/10.1016/j.coldregions.2019.03.014.

Placidi, L., Hutter, K., Faria, S.H., 2006. A critical review of the mechanics of polycrystalline polar ice. GAMM-Mitt. 29 (1), 80–117.

Reiner, M., 1945. A mathematical theory of dilatancy. Am. J. Math. 67 (3), 350–362.

Rivlin, R.S., 1947. Hydrodynamics of non-Newtonian fluids. Nature 160 (4070), 611.

Schwarzl, F., Staverman, A.J., 1952. Time-temperature dependence of linear viscoelastic behaviour. J. Appl. Phys. 23, 838–843.

Smith, G., Morland, L.W., 1981. Viscous relations for the steady creep of polycrystalline ice. Cold Reg. Sci. Technol. 5, 141–150.

Spring, U., Morland, L.W., 1982. Viscoelastic solid relations for the deformation of ice. Cold Reg. Sci. Technol. 5, 221–234.

Spring, U., Morland, L.W., 1983. Integral representations for the viscoelastic deformation of ice. Cold Reg. Sci. Technol. 6, 185–193.

Staroszczyk, R., 2019. Ice Mechanics for Geophysical and Civil Engineering Applications. Springer Nature, Cham, Switzerland.

Staroszczyk, R., Gagliardini, O., 1999. Two orthotropic models for the strain-induced anisotropy of polar ice. J. Glaciol. 45 (151), 485–494.

Staroszczyk, R., Morland, L.W., 1999. Orthotropic viscous model for ice. In: Hutter, K., Wang, Y., Beer, H. (Eds.), Advances in Cold-Region Thermal Engineering and Sciences. Springer, Berlin, pp. 249–258.

Staroszczyk, R., Morland, L.W., 2000. Orthotropic viscous response of polar ice. J. Eng. Math. 37, 191–209.

Svendsen, B., Hutter, K., 1996. A continuum approach for modelling induced anisotropy in glaciers and ice sheets. Ann. Glaciol. 23, 262–269.

Thorsteinsson, T., Kipfstuhl, J., Miller, H., 1997. Textures and fabric in the GRIP ice core. J.Geophys.Res. 102 26583–25599.